Bioassay of prostate-specific antigen (PSA) using microcantilevers

Guanghua Wu[1], Ram H. Datar[2], Karolyn M. Hansen[3], Thomas Thundat[3], Richard J. Cote[2], and Arun Majumdar[1]*

Diagnosis and monitoring of complex diseases such as cancer require quantitative detection of multiple proteins. Recent work has shown that when specific biomolecular binding occurs on one surface of a microcantilever beam, intermolecular nanomechanics bend the cantilever, which can be optically detected. Although this label-free technique readily lends itself to formation of microcantilever arrays, what has remained unclear is the technologically critical issue of whether it is sufficiently specific and sensitive to detect disease-related proteins at clinically relevant conditions and concentrations. As an example, we report here that microcantilevers of different geometries have been used to detect two forms of prostate-specific antigen (PSA) over a wide range of concentrations from 0.2 ng/ml to 60 μg/ml in a background of human serum albumin (HSA) and human plasminogen (HP) at 1 mg/ml, making this a clinically relevant diagnostic technique for prostate cancer. Because cantilever motion originates from the free-energy change induced by specific biomolecular binding, this technique may offer a common platform for high-throughput label-free analysis of protein–protein binding, DNA hybridization, and DNA–protein interactions, as well as drug discovery.

It is becoming increasingly evident that high-throughput identification and quantitation of a large number of biological molecules is important for generating a molecular profile that is critical in diagnosis, monitoring, and prognostic evaluation of complex diseases such as cancer[1,2]. For genetic analysis, commercially available nucleic acid microarrays allow sensitive identification of thousands of DNA sequences simultaneously. For protein analysis, which is directly relevant for disease detection, high-throughput diagnostics has, however, remained a challenge. Multiplexed protein analysis techniques currently used can be broadly divided into four different categories: (1) radioactive, chemiluminescent, or fluorescent reporting of antigen–antibody binding[3–5]; (2) time-of-flight mass spectroscopy[6]; (3) electrophoretic separation[7]; and (4) detection of changes in surface properties due to antigen–antibody binding[8–15]. Although they all have their individual strengths, they currently suffer either from the inability to identify or quantitate proteins[7], or nonspecific binding of a serum analyte to the sensor surface[16]. Truly universal label-free biosensors for sensitive and specific detection of protein analytes in a high-throughput fashion are not yet a reality.

Recent papers have reported the observation that when specific biomolecular interactions occur on one surface of a microcantilever beam, the cantilever bends[17–20] (see Fig. 1). The recent discovery of the origin of nanomechanical motion generated by DNA hybridization and protein–ligand binding[19] provided some insight into the specificity of the technique. In addition, its use for DNA–DNA hybridization detection, including accurate positive/negative detection of one–base pair mismatches, was also reported[19,20]. Besides being label free, this technology readily lends itself to formation of microarrays using well-known microfabrication techniques[21], thereby offering the promising prospect of high-throughput protein analysis. What has remained unclear, however, is whether this technique has sufficient specificity and sensitivity to be used for the detection of disease-related proteins at clinically relevant conditions and concentrations. To address this technologically critical issue, we demonstrate in this paper the application of this technique for sensitive and specific detection of PSA as an example of both protein–protein binding in general and tumor marker detection in particular.

Prostate cancer is currently the most prevalent form of cancer in men and the second leading cause of male cancer death in the United States. PSA that is detectable in serum has proved to be an extremely useful marker for early detection of prostate cancer and in monitoring patients for disease progression and the effects of treatment. PSA is a 33–34 kDa glycoprotein with chymotrypsin-like protease activity. This enzymatically active form of PSA forms complexes with the serum protease inhibitor α_1-antichymotrypsin (ACT) to create the predominant form of PSA in serum. PSA also forms a complex with α_2-macroglobulin (A2M) and other serum enzyme inhibitors, but to a much lesser degree[22,23]. The PSA test is limited by its relative lack of accuracy in men whose PSA levels fall in the "diagnostic gray zone" of 4–10 ng/ml. The distinction between complexed PSA (cPSA) and unbound or free PSA (fPSA), however, has become recognized as a clinically relevant feature of the PSA tests. Thus, although approximately 75–85% of PSA exists as cPSA in benign prostatic hypertrophy (BPH), the proportion increases to lie between 90 and 100% in prostate cancer; thus the lower the fPSA in serum, the higher are the chances of malignancy. Most newer diagnostic assays take this into account by incorporating dual labels for simultaneous and equimolar measurement of fPSA and cPSA. Although there are controversies regarding the frequency of screening, proponents of PSA-based prostate cancer screening maintain that early detection is the closest thing currently to a cure[24]. Most of the current PSA assays are variations of enzyme-linked immunosorbent assays (ELISA), differing in detection by virtue of either enzymatic, fluorescent, or chemiluminescent labels, which report on the specific formation of PSA immune complex.

[1]*Department of Mechanical Engineering, University of California, Berkeley, CA 94720.* [2]*Department of Pathology, University of Southern California, Los Angeles, CA 90033.* [3]*Life Sciences Division, Oak Ridge National Laboratory, Oak Ridge, TN 37831.* **Corresponding author (majumdar@me.berkeley.edu).*

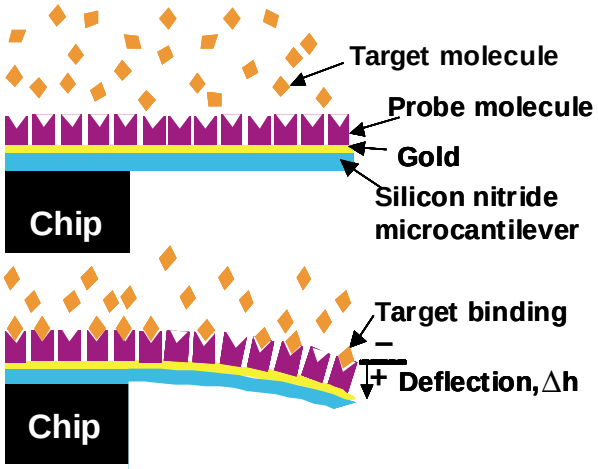

Figure 1. Diagram of interactions between target and probe molecules on cantilever beam. Specific biomolecular interactions between target and probe molecules alter the intermolecular nanomechanical interactions within a self-assembled monolayer on one side of a cantilever beam. This can produce a sufficiently large force to bend the cantilever beam and generate motion.

Generally, two distinct monoclonal antibodies directed against different PSA epitopes are used in a "sandwich assay" format for capture and detection, which enhances the specificity.

In this paper, we have used a polyclonal anti-PSA antibody as a "ligand" covalently linked to the cantilever surface. The cantilever deflection due to specific fPSA binding with this antibody allows us to detect fPSA concentrations from 0.2 ng/ml to 60 μg/ml, which includes the clinically relevant diagnostic PSA concentration range. We have been able to detect fPSA even against the simulated background "noise" of unrelated human serum proteins such as HP and HSA or nonhuman serum protein such as bovine serum albumin (BSA), which were present at concentrations as high as 1 mg/ml. This indicates that we have been able to largely alleviate the problem of nonspecific binding and assay interference due to the nontarget analytes. We have also been able to attain similar specificity and range of sensitivity with cPSA.

Results and discussion

Figure 2A shows the cantilever deflection as a function of time for different concentrations of fPSA in a mixture with 1 mg/ml of BSA as background. The cantilevers used (see Fig. 6) in this set of experiments (Figs 2, 3) were made of silicon nitride (SiN_x) with a thin coating of gold on one side and with a length of 200 μm, thickness of 0.5 μm, and each leg 20 μm wide. The gold film was used to immobilize the PSA antibody to the cantilever through thiol chemistry (see Experimental Protocol). With PSA antibody immobilized on the bottom gold surface of the cantilever, the cantilever was found always to bend up as a result of antigen–antibody binding. This is caused by the increased intermolecular repulsion between the antigen–antibody complexes on the cantilever surface. It is evident that over a time period of 3–4 h, the cantilever deflection increased and then saturated to a steady-state value. The long detection time is caused either by diffusion of molecules in the fluid cell or through conformational relaxation of the antigen–antibody complex on the cantilever surface[25]. The diffusion time scale, $\tau = L^2/2D$, for a fluid cell size of $L \approx 0.1$ cm and PSA diffusion coefficient $D \approx 8.5 \times 10^{-7}$ cm^2/s (see Experimental Protocol), is on the order of 100 min, which is the time scale observed, making diffusion the likely candidate for the long detection time. The diffusion can be significantly enhanced by proper microfluidic design currently underway. The steady-state deflection was found to be related to the fPSA concentration in the solution. To check whether the deflection was caused by antigen–antibody specific binding, cantilevers containing no PSA antibody were exposed to a mixture containing 60 μg/ml of fPSA and 1 mg/ml of BSA, and the deflection was found to be negligible (see Fig. 2A). On the other hand, when cantilevers functionalized with PSA antibody were exposed to 1 mg/ml of only BSA without any fPSA, no significant cantilever deflection was observed, also indicating the high specificity of this technique. Similarly, Figure 2B shows the cantilever deflection as a function of time for different concentration of fPSA in a mixture of HSA and HP as background. To check for specificity, we again exposed fPSA to a cantilever without any PSA antibody and found negligible deflection. When a can-

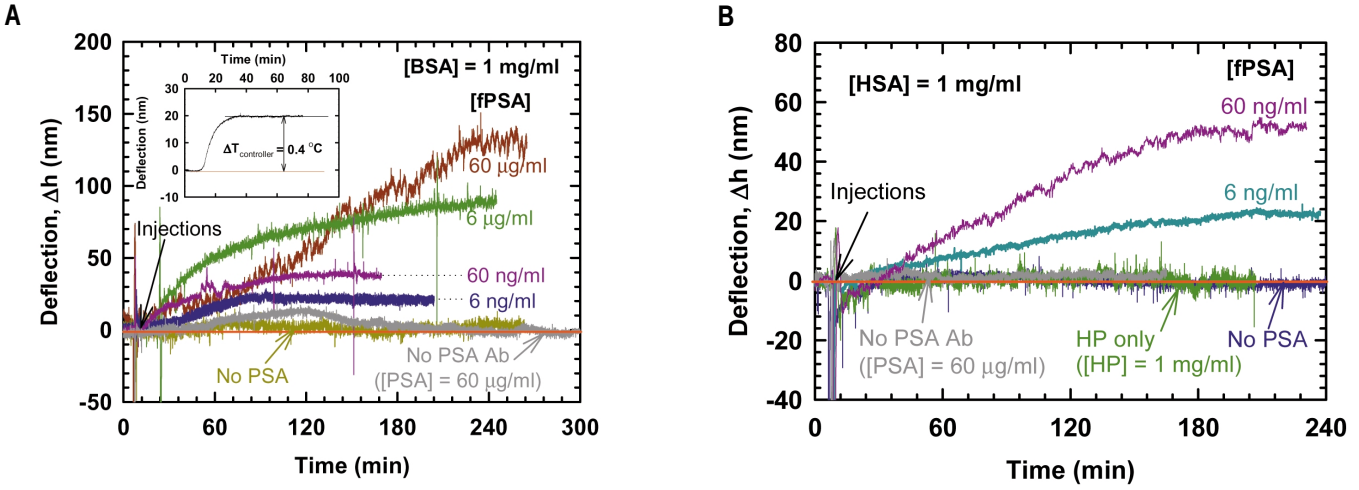

Figure 2. Detection of free PSA (fPSA). (A) Cantilever deflection versus time for fPSA detection sensitivity against a background of 1 mg/ml of BSA using 200-μm-long and 0.5-μm-thick silicon nitride microcantilevers. fPSA detection was feasible over a concentration range 6 ng/ml to 60 μg/ml using this cantilever geometry. Note the lack of deflection in the absence of both the ligand (anti-PSA antibody) and the ligate (fPSA). The inset plots cantilever deflection for a 0.4°C temperature change of the system and shows that the thermal stability is within the noise of the system. (B) Specificity of fPSA detection against a high background of human serum proteins, namely, human serum albumin (HSA) and human plasminogen (HP), both at concentrations of 1 mg/ml. The cantilevers used were 200 μm long and 0.5 μm thick and made of silicon nitride.

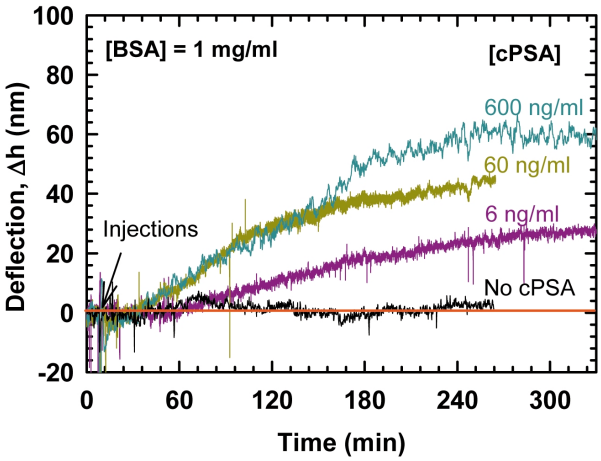

Figure 3. Detection of complex PSA (cPSA).Cantilever deflection versus time for detection of cPSA in presence of 1 mg/ml of BSA using 200-µm-long and 0.5-µm-thick silicon nitride microcantilevers. The microcantilever deflections for 6 ng/ml and 60 ng/ml of cPSA are slightly larger than those for fPSA at the same concentrations.

tilever functionalized with PSA antibody was exposed to HSA and HP in the absence of fPSA, again no significant cantilever deflection was observed. This indicated the high specificity between fPSA antigen–antibody binding in the background of HSA and HP.

Figure 3 shows the cantilever deflection as a function of time for different concentrations of cPSA with 1 mg/ml BSA as background. The cantilever deflection increases with concentration of cPSA within the range studied. The control experiment in which no cPSA was used shows very small signal, indicating the high specificity of binding between cPSA and PSA antibody. The magnitude of the deflection is slightly larger for cPSA–PSA antibody binding than that for fPSA–PSA antibody binding at the same concentration, indicating slightly better sensitivity for cPSA.

The reason for this high specificity is that cantilever motion originates[19] from the change in surface free energy of one surface of the cantilever and not the other. Because specific binding between molecules leads to much higher free-energy change than for nonspecific binding, cantilever deflections are a response to specific binding. The value of the cantilever deflection, Δh, can be estimated from Stoney's formula[17]

$$\Delta h = 3\sigma(1-\nu)/E \bullet (L/d)^2 \qquad (1)$$

where σ is the change in surface free-energy density (or surface stress) due to specific binding, E is the elastic modulus of the cantilever material ($\approx 1.8 \times 10^{11}$ N/m^2 for silicon nitride), ν is its Poisson ratio ($\approx$0.3 for silicon nitride), and L and d are the length and the thickness of the cantilever, respectively. It is clear that longer and thinner cantilevers would produce larger deflections for the same value of surface stress. Figure 4 shows the steady-state cantilever deflections as a function of PSA concentration in a BSA background for different lengths, L, and thicknesses, d, of cantilevers. Using 200-µm-long and 0.5-µm-thick cantilevers, the lowest fPSA concentration that we could clearly detect above noise was 6 ng/ml. However, when we used 600-µm-long and 0.65-µm-thick SiN_x cantilevers, fPSA concentration as low as 0.2 ng/ml was detectable. This is close to the resolution required for PSA-based diagnosis of prostate cancer[24]. Also shown in Figure 4 is the steady-state cantilever deflection as a function of the cPSA concentration with 1 mg/ml BSA as background. At the same concentration, the slightly larger magnitude of the deflection than that for fPSA suggests the slightly better sensitivity for cPSA.

Because cantilever deflections depend on both the surface stress and geometry, deflections alone cannot be used for PSA assay. One must obtain a geometry-independent quantity, which depends only on PSA concentration. Because the origin of cantilever deflection lies in the generation of surface stress, σ must be fundamentally related to PSA antigen–antibody binding. Assuming that the number of PSA antigen–antibody binding sites per unit surface area is related to PSA concentration in the analyte solution, one would expect σ to be related to PSA concentration, regardless of the cantilever geometry. Using the formula in Eq. (1), we calculated σ based on the deflections in Figure 4 for different cantilever thicknesses and lengths. Figure 5 plots σ as a function of PSA concentration, which clearly indicates that the data in Figure 4 from different cantilevers collapses to a single curve, supporting our hypothesis that the surface stress, σ, is fundamentally related to PSA concentration in the analyte. This now forms the foundation for a PSA assay based on microcantilevers.

The high specificity and sensitivity of the nanomechanical bioassay demonstrated here, combined with the ability to create cantilever arrays using low-cost semiconductor microfabrication processes[21], makes this technology an ideal platform for high-throughput and label-free analysis of proteins. We describe here its clinical relevance through sensitive detection and quantification of an important diagnostic biomolecule, PSA. PSA is currently detected using ELISAs, which are sensitive and have a relatively low cost per test. However, there are several important differences between ELISA and the nanomechanical assay described here. ELISA reactions require multiple steps, each with separate reagents. Each ELISA analysis requires a separate distinct reaction and, in addition, requires a label for detection of the analyte. The nanomechanical assay described here needs no label and can be performed in a single reaction without

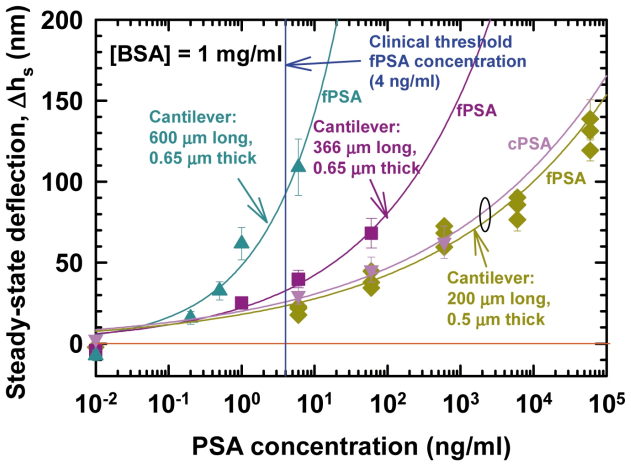

Figure 4. Steady-state cantilever deflections as a function of fPSA and cPSA concentrations for three different cantilever geometries. Note that longer cantilevers produce larger deflections for the same PSA concentration, thereby providing higher sensitivity. Using 600-µm-long and 0.65-µm-thick silicon nitride cantilevers, it was feasible to detect fPSA concentration of 0.2 ng/ml. Every data point on this plot represents an average of cantilever deflections obtained in multiple experiments done with different cantilevers, whereas the range of deflections obtained from these experiments is shown as the error bar. The only exception is the data for fPSA detection using 200 µm cantilevers, where the data (green diamonds) from multiple experiments at a given concentration is shown as a cluster plot. The error bar in each of these data points represents the fluctuation of the cantilever during the particular measurement.

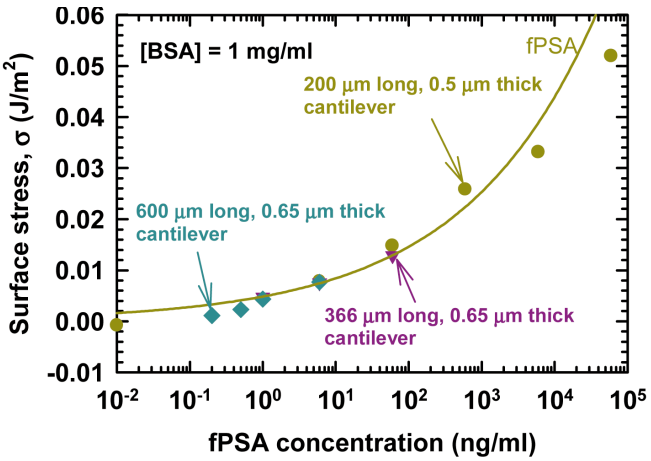

Figure 5. Surface stress as a geometry-independent parameter for assaying PSA. The data for cantilever deflections for different cantilever geometries collapse onto a single curve for surface stress as a function of fPSA concentration.

additional reagents. Moreover, an array of microcantilevers can be used to perform multiple assays by, for example, coating each cantilever with a different antibody. The potential advantages of a label-free assay that can measure multiple analytes in a single step without addition of other reagents are enormous, and could ultimately translate to a much lower cost per test. For example, this could increase the general availability of multiple serum tumor marker screening, which is currently cost prohibitive. The ability to vary the cantilever length and thickness can enable both high resolution as well as a high dynamic range, as exemplified in this study. We note here that despite being able to detect PSA at the current limit of ELISA (0.2 ng/ml), there is room for further improvement in sensitivity either through controlling the roughness[26] of the gold surface or by controlling the surface density of probe molecules[27]. The label-free option makes it particularly attractive for drug discovery, which requires one to detect specific binding between small molecules with proteins. The utility of this technique in detecting DNA hybridization[17,19,20] makes it a common platform for detecting both DNA and proteins, as well as DNA–protein interactions. We, in fact, suggest that because cantilever motion is driven by free-energy change, which is at the heart of all specific biomolecular binding, this technique is sufficiently general to detect many specific biomolecular interactions without the need of labels.

Experimental protocol

Experimental setup. A diagram of the experimental setup is given in Figure 6. A low-power He-Ne laser (~3 mW power) is focused onto the tip of the cantilever. The laser beam reflected off the cantilever is directed into a position-sensitive diode (PSD) that can detect the vertical position of a laser beam. A fluid cell—commercially available from Digital Instruments (DI; Santa Barbara, CA)—within which the cantilever is mounted, forms a 100 µl liquid cavity on a glass slide with a Teflon O-ring between them. The 200-µm-long, 40-µm-wide, and 0.5-µm-thick V-shaped micromechanical silicon nitride cantilevers (see Fig. 6) were purchased from DI, whereas longer diving board–shaped cantilevers were microfabricated in the Berkeley Microfabrication Laboratory. Because the cantilevers contained gold and SiN_x, which have different thermal expansion coefficients, temperature changes could actuate the cantilever as well. To eliminate this effect, a thermoelectric cooler and a temperature controller are used to control the temperature of the liquid cavity within ±0.05°C. The inset in Figure 2A shows the thermal stability of the system, where the cantilever deflection is plotted for a controlled 0.4°C temperature change.

Reagents. Dithiobis(sulfosuccinimidylpropionate) (DTSSP), obtained from Pierce Chemical Company (Rockford, IL), is a water-soluble, homobifunctional *N*-hydroxysuccimide (NHS) ester. It is thiol-cleavable and widely used for conjugating radiolabeled ligands to cell surface receptors[28–30].

Rabbit Anti-Human Prostate-Specific Antigen (RAH-PSA) antibody was procured from DAKO (Carpinteria, CA). fPSA and cPSA (>95% purity, purified by sodium dodecyl sulfate–polyacrylamide gel electrophoresis) were obtained from CalBioChem (La Jolla, CA). Affinity-purified BSA was ordered from Pierce Chemical Company. HSA and HP were bought from Academy Biomedical (Houston, TX). Other chemicals were purchased from Sigma-Aldrich (St. Louis, MO).

Cantilever functionalization. *Cleaning procedure.* The original gold and chromium coatings from the silicon nitride cantilevers were stripped off using gold and chromium etchants. A fresh layer of 25-nm-thick gold film was then evaporated on one side of the cantilever. To improve the adhesion of gold to silicon nitride, a 5-nm-thick chromium layer was evaporated onto the cantilever surface first. The cantilever was sequentially cleaned in methanol, acetone, and isopropanol-2 for 10 min each. This was followed by a quick 1 min "piranha dip" (H_2O_2: H_2SO_4 = 1:3) for each cantilever. Finally, each cantilever was rinsed with deionized water for 10 min. This process was done immediately before the experiments. The fluid cell and glass slide were cleaned using standard detergent for glassware and rinsed with large amounts of deionized water for about 5 min.

Functionalizing cantilever with DTSSP. DTSSP was dissolved in 5 mM sodium citrate buffer (pH = 5.0) at a concentration of 1.5 mM just before use because DTSSP is moisture-sensitive. Cantilevers immersed in this solution for about 2 h at room temperature results in strong adherence of DTSSP to the gold surface by a disulfide linkage[31].

Immobilizing RAH-PSA. After derivatizing with DTSSP, the cantilevers were rinsed with 20 mM sodium phosphate buffer, 0.15 M NaCl and pH 7.5 (PBS) for 5 min and then immersed in RAH-PSA solution for at least 5 h at room temperature. RAH-PSA was purified using D-Salt Excellulose plastic desalting columns (Pierce) to remove the vendor-added solvent and dissolved in PBS to a concentration of 160 µg/ml.

Saturating with BSA (or HSA). Following the immobilization of RAH-PSA onto the cantilever surface, the cantilever was washed by 1 mg/ml BSA solution in PBS (BSA/PBS) thrice for about 10 min and stored in BSA–PBS solution overnight at room temperature. This step is similar for the case of HSA in which one substitutes HSA for BSA.

Test procedure. Free PSA was purified with the BSA–PBS (or HSA–PBS) solution using D-Salt Excellulose desalting columns to remove the vendor-added solvent. The final solution was aliquoted and diluted to concentrations covering several orders of magnitude extending from 0.1 to

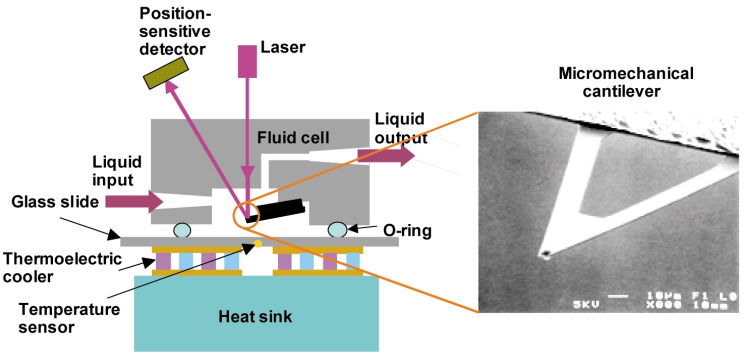

Figure 6. Schematic diagram of the experimental setup showing a fluid cell within which a microcantilever beam was mounted. The scanning electron micrograph on the right shows the geometry of a gold-coated silicon nitride cantilever beam that was 200 µm long, 0.5 µm thick, and with each leg 40 µm wide. To measure the cantilever deflection, a laser was reflected off the back of the cantilever and focused onto a position-sensitive detector. The reagents were injected into the fluid cell using the liquid ports. The fluid cell was mounted on a temperature-controlled glass slide.

60,000 ng/ml. The functionalized cantilever was mounted onto the fluid cell and equilibrated in BSA–PBS solution until a stable baseline of cantilever deflection was obtained (usually around 2 h). The control (such as BSA–PBS, HSA–PBS, HP–PBS) or analyte (fPSA or cPSA) was then injected into the fluid cell and cantilever deflection was monitored *in situ*. All the experiments were carried out at controlled temperature of 28.0 ± 0.05°C. Because there was no flow through the fluid chamber, the reaction happened in a static environment by molecular diffusion to the cantilever surface and then binding to the probes. The diffusion coefficient of the solute molecules is $D = k_B T/f$, where k_B is the Boltzmann constant (1.38×10^{-23} J/K), T is the absolute temperature, and f is the frictional coefficient of the molecule given as $f = 6\pi\eta(3V_h/4\pi)^{1/3}$. Here, η is the viscosity of the solvent (8.55×10^{-4} Ns/m^2), $V_h = M(V_2 + \delta_1 V_1)/N_0$ is the volume of the hydrated molecule; M is the molecular weight of the solute molecule with the units g/mol; N_0 is Avogadro's number; δ_1 is the hydration (grams of H_2O bound per gram of solute, for protein, $\delta \approx 0.3$); V_1 is the partial specific volume of H_2O (≈1 cm^3/g); V_2 is the partial specific volume of the solute (typical values for proteins: 0.69–0.75 cm^3/g). For PSA, M = 34,000 g/mol, $D = 8.5 \times 10^{-7}$ cm^2/s.

Acknowledgments

This work was supported by the Innovative Molecular Analysis Technologies (IMAT) program of the National Cancer Institute (NIH) (Grant R21 CA86132). G.W. and A.M. would also like to thank the Engineering Program of the DOE Basic Energy Sciences (Grant DE-FG03-98ER14870). K.H., H.J., and T.T. were supported by the Office of Biological and Environmental Research (OBER), US Department of Energy under contract DE-AC05-96OR22464 with Oak Ridge National Laboratory, managed by Lockheed Martin Energy Research Corporation.

Received 17 January 2001; accepted 29 June 2001

1. Emmert-Buck, M.R. *et al.* Molecular profiling of clinical tissue specimens: feasibility and applications. *Am. J. Pathol.* **156**, 1109–1115 (2000).
2. Sander, C. Genomic medicine and the future of health care. *Science* **287,** 1977–1978 (2000).
3. Whelan, J.P., Kusterbeck, A.W., Wemhoff, G.A., Bredehorst, R. & Ligler, F.S. Continuous flow immunosensor for detection of explosives. *Anal. Chem.* **65**, 3561–3565 (1993).
4. Devine, P.J. *et al.* A fiberoptic cocaine biosensor. *Anal. Biochem.* **227**, 216–224 (1995).
5. Zhu, H. *et al.* Analysis of yeast protein kinases using protein chips. *Nat. Genet.* **26**, 283–289 (2000).
6. Davies, H., Lomas, L. & Austen, B. Profiling of amyloid beta peptide variants using SELDI protein chip arrays. *Biotechniques* **27**, 1258–1261 (1999).
7. Heegaard, N.H. & Kennedy, R.T. Identification, quantitation and characterization of biomolecules by capillary electrophoretic analysis of binding interactions. *Electrophoresis* **20**, 3122–3133 (1999).
8. Mullett, W., Lai, E.P. & Yeung, J.M. Immunoassay of fumonisins by a surface plasmon resonance biosensor. *Anal. Biochem.* **258**, 161–167 (1998).
9. Rubio, I., Buckle, P., Trutnau, H. & Wetzker, R. Real-time assay of the interaction of a GST fusion protein with a protein ligate using resonant mirror technique. *Biotechniques* **22**, 269–271 (1997).
10. Nicholson, S., Gallop, J.L., Law, P., Thomas, H. & George, A.J. Monitoring antibody responses to cancer vaccination with a resonant mirror biosensor. *Lancet* **353**, 808 (1999).
11. Ostroff, R.M. *et al.* Fixed polarizer ellipsometry for simple and sensitive detection of thin films generated by specific molecular interactions: applications in immunoassays and DNA sequence detection. *Clin. Chem.* **44**, 2031–2035 (1998).
12. Piehler, J. *et al.* Label-free monitoring of DNA–ligand interactions. *Anal. Biochem.* **249**, 94–102 (1997).
13. Jones, V.W., Kenseth, J.R., Porter, M.D., Mosher, C.L. & Henderson, E. Microminiaturized immunoassays using atomic force microscopy and compositionally patterned antigen arrays. *Anal. Chem.* **70**, 1233–1241 (1998).
14. Blonder, R. *et al.* Application of redox enzymes for probing the antigen–antibody association at monolayer interfaces: development of amperometric immunosensor electrodes. *Anal. Chem.* **68**, 3151–3157 (1996).
15. Dahint, R., Bender, F. & Morhard, F. Operation of acoustic plate mode immunosensors in complex biological media. *Anal. Chem.* **71**, 3150–3156 (1999).
16. Bock, J.L. The new era of automated immunoassay. *Am. J. Clin. Pathol.* **113**, 628–646 (2000).
17. Fritz, J. *et al.* Translating biomolecular recognition into nanomechanics. *Science* **288**, 316–318 (2000).
18. Raiteri, R., Nelles, G., Butt, H.-J., Knoll, W. & Skladal, P. Sensing of biological substances based on the bending of microfabricated cantilevers. *Sensors and Actuators B* **61**, 213–217 (1999).
19. Wu, G. *et al.* Origin of nanomechanical cantilever motion generated from biomolecular interactions. *Proc. Natl. Acad. Sci. USA* **98**, 1560–1564 (2001).
20. Hansen, K.M. *et al.* Cantilever-based optical deflection assay for discrimination of DNA single nucleotide mismatches. *Anal. Chem.* **73**, 1567–1571 (2001).
21. Madou, M. *Fundamentals of microfabrication*. (CRC Press, New York; 1997).
22. Christensson, A. *et al.* Serum prostate specific antigen complexed to α_1-antichymotrypsin as an indicator of prostate cancer. *J. Urol.* **150**, 100–105 (1993).
23. Lilja, H. Significance of different molecular forms of serum PSA. *Urol. Clin. North Am.* **20**, 681–686 (1993).
24. Polascik, T.J., Oesterling, J.E. & Partin, A.W. Prostate specific antigen: a decade of discovery—what we have learned and where we are going. *J. Urol.* **162**, 293–306 (1999).
25. Moulin, A.M., O'Shea, S.J. & Welland, M.E. Micro-cantilever biosensors. *Ultramicroscopy* **82**, 23–31 (2000).
26. Lavrik, N.V. *et al.* Enhanced chemi-mechanical transduction at nanostructured interfaces. *Chem. Phys. Lett.* **336**, 371–376 (2001).
27. Ji, H.F. *et al.* A novel self-assembled monolayer (SAM) coated microcantilever for low level caesium detection. *Chem. Commun.* **6**, 457–458 (2000).
28. Staros, J.V. *N*-Hydroxysulfosuccinimide active esters: bis(*N*-hydroxyssuccinimide) esters of two dicarboxylic acids are hydrophilic, membrane impermeant, protein crosslinkers. *Biochemistry* **21**, 3950–3955 (1982).
29. Knoller, S., Shpungin, S. & Pick, E. The membrane-associated component of the amphiphile-activated, cytosol-dependent superoxide-forming NADPH oxidase of macrophages is identical to cytochrome b559. *J. Biol. Chem.* **266**, 2795–2804 (1991).
30. Waugh, S.M., DiBella, E.E. & Pilch, P.F. Isolation of a proteolytically derived domain of the insulin receptor containing the major site of crosslinking/binding. *Biochemistry* **28**, 3448–3455 (1989).
31. Katz, E.Y. A chemically modified electrode capable of a spontaneous immobilization of amino compounds due to its functionalization with succinimidyl groups. *J. Electroanal. Chem.* **291**, 257–260 (1990).